FUDMA Journal of Sciences (FJS)
ISSN online: 2616-1370
ISSN print: 2645 - 2944
Vol. 9 No. 6, June, 2025, pp 38 – 44
DOI: https://doi.org/10.33003/fjs-2025-0906-3672

SIMULATION OF A SECURE COMMUNICATION SCHEME VIA HYBRID SYNCHRONIZATION OF CHAOTIC SYSTEMS WITH MINIMAL CONTINUOUS CHAOS

***[1]Oyeleke, Kehinde S., [2]Ojo, Kayode S., [3]Adeniji, Abidemi E. and [4]Odumuyiwa, Victor T.**

[1]Department of Physical Sciences, Lagos State University of Science and Technology, Ikorodu, Lagos, Nigeria.
[2]Department of Physics, University of Lagos, Lagos, Nigeria.
[3]Department of Physical Sciences, Bells University of Technology, Ogun state, Nigeria.
[4]Department of Computer Science, University of Lagos, Lagos, Nigeria.

*Corresponding authors' email: oyelek.ks@lasustech.edu.ng Phone: +2348037850388

ABSTRACT
This paper uses the Rossler attractor as a classical oscillator and presents a secure communication approach based on the hybrid synchronization of two identical chaotic systems via Lyapunov direct method. Equilibrium and bifurcation are two examples of fundamental dynamical features that are examined. A secure communication scheme is also presented based on synchronizing evolving chaotic systems with an uncertain parameter. The chaotic transmitter, the modulation, the chaotic receiver and the demodulation make up the communication scheme. The message signal is modulated into the system via the modulation process. Next, a public channel is used to transmit the chaotic signals to the recipient. The receiver end achieves synchronization between the transmitter and the receiver systems; and simultaneously estimates the unknown parameter through the design of the controller and parameter update law. The message signal is retrieved using the suitable demodulation technique and the detected parameter. To show the viability and validity of the described secure communication scheme, numerical simulations are performed.

Keywords: Secure communication, Chaos system, Lyapunov direct method, Message signal

INTRODUCTION

Research on chaotic system synchronization has expanded significantly since the ground breaking work of Pecora and Carroll (1990). Numerous synchronization occurrences in chaotic systems have been reported until now, such as complete synchronization (Pecora & Carroll, 1990), generalized synchronization (Zheng & Hu, 2000), phase synchronization (Rosenblum *et al.*, 1996), projective synchronization (Li & Xu, 2004) etc. It has also attracted a lot of research attention because of its relevant practical applications (Boccaletti *et al.*, 2002). It is being applied to secure communication systems in which the intended chaotic signal in the transmitter is modulated and the original signal is then demodulated in the received signal in the receiver end (Cuomo & Oppenheim, 1993; Kocarev & Parlitz, 1995; Yau *et al.*, 2012). Essentially, the novel idea for transmitting a message signal through chaotic systems is that a message signal is implanted in the transmitter system, which generates a chaotic signal. Eventually, the receiver recovers the message signal via a public channel and then, decodes the message signal.

Secure communication systems have been studied using a variety of techniques (Rulkov & Tsimring, 1999; Li *et al.*, 2003; Miliou *et al.*, 2007; Yeh & Wu, 2008; Lu *et al.*, 2008; Zhao *et al.*, 2014; Wu *et al.*, 2015; Olusola *et al.*, 2020). Also, three different case studies on chaos-based secure communication systems were presented by Zaher and Abu-Rezq (2011); brain-emotional learning has been used to study a secure communication system through chaos synchronization (Samimi *et al.*, 2020). A secure communication scheme that is based on a new hyperchaotic system with three quadratic nonlinearities was presented by Benkouider *et al.* (2022). Recently, a scientific study using the Current Feedback Amplifier and Op-Amp to realize a chaotic oscillator and apply it to secure communication was published (Rai *et al.*, 2023). Also, hybrid synchronization has found its applications in signal processing and secure communication (Trikha & Jahanzaib, 2021; Bouraoui & Kemih, 2013; Ni-huan & Zhi-hong, 2012).

To lower the suspicion of an intending intruder as well as make the intrusion more difficult, we use a system with minimal continuous chaos and a hybrid synchronization scheme in this study.

System Description and Dynamical Analyses

System Description

We consider the original system presented by Rossler (1976), which can be described by following autonomous differential equations:

$$\begin{cases} \dot{x}_1 = -(x_2 + x_3) \\ \dot{x}_2 = x_1 + a x_2 \\ \dot{x}_3 = \mathrm{b} + x_3(x_1 - c), \end{cases} \qquad (1)$$

where a, b and c are real constant parameters that determine the behaviour of the system. The values first studied by Rossler (976) are $a = b = 0.2$ and $c = 5.7$. x_1, x_2 and x_3 are the three variables which evolve with time. The first two expressions in Equation (1) have linear terms that cause oscillations in the variables x_1 and x_2. The last expression has only one nonlinear term $x_1 x_3$, hence the system is expected to exhibit chaotic behaviour.

This system has minimal continuous chaos for at least three reasons: (i) it has a single quadratic term, which reduces nonlinearity; (ii) a chaotic attractor is generated, which has one lobe as opposed to the two lobes of the Lorenz attractor; and (iii) its phase-space has the minimum dimension of three (Gaspard, 2005). With parameter values $a = b = 0.2$ and $c = 5.7$ (Gosar, 2011) and initial condition $(0, 0, 0)$; the phase space is as shown in Figure 1.

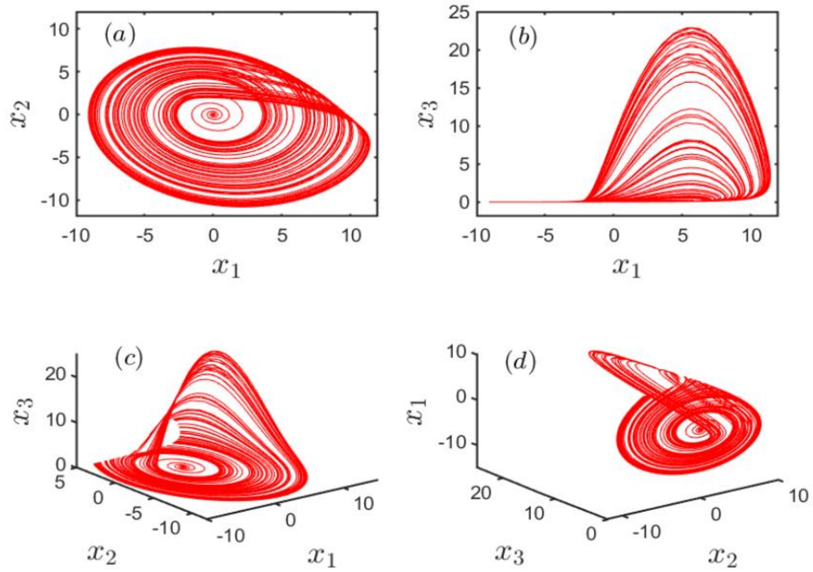

Figure 1: Phase portrait of the Rossler attractor with the following parameters $a = 0.2, b = 0.2, c = 5.7$

The divergence of Equation (1) is in the form:

$$\begin{cases} \Delta V = \frac{d\dot{x}_1}{dx_1} + \frac{d\dot{x}_2}{dx_2} + \frac{d\dot{x}_3}{dx_3} \\ \Delta V = a - c \end{cases} \quad (2)$$

Obviously, for the parameter values considered, $\Delta V < 0$. Consequently, Equation (1) is dissipative (Olusola *et al.*, 2020; Benkouider *et al.,* 2022). Also, the equilibria of Equation (1) can be obtained by solving:

$$\begin{cases} -x_2 - x_3 = 0 \\ x_1 + ax_2 = 0 \\ \mathrm{b} + x_1x_3 - cx_3 = 0. \end{cases} \quad (3)$$

By linearizing the system around equilibrium point $E_0(0,0,0)$, it results in the following Jacobian matrix:

$$J = \begin{vmatrix} 0 & -1 & -1 \\ 1 & a & 0 \\ x_3 & 0 & (x_1 - c) \end{vmatrix} \quad (4)$$

The eigenvalues can be determined by solving the following cubic Equation:

$$\lambda^3 - \lambda^2(a + x_1 - c) + \lambda(ax_1 - ac + x_3 + 1) - x_1 + c - ax_3 = 0. \quad (5)$$

For the centrally located fixed point and parameter value $a = 0.2, b = 0.2$,and $c = 5.7$, Equation (5) yields eigenvalues of: $\lambda_{1,2} = 0.1000 \pm 0.9950i$, $\lambda_3 = -5.7000$.

Dynamical Analysis

Dynamical properties of a dynamic system can be examined by the bifurcation diagram and the Lyapunov exponents spectrum. In this work, the bifurcation of Equation (1) against a varied parameter c is examined; using MATLAB Simulink, the result as well as the Lyapunov exponent is shown in Figure 2. Figure 2a and Figure 2b depict the bifurcation diagram and the Lyapunov exponents spectrum respectively. Figure 2c is a zoomed version of Figure 2b showing only the first and the second Lyapunov exponents.

The value of c varies from 0.5 to 6.5. The behaviour in Figure 2a shows that when $0.5 \leq c \leq 2.4$, the dynamic is periodic. For $2.4 \leq c \leq 3.6$, the period-doubling behaviour of the system is observed. At $3.6 \leq c \leq 4.1$, the system has a second-period doubling behaviour, and finally, the chaos behaviour region starts from $c \geq 4.1$. Each bifurcation dynamic is corroborated with the Lyapunov exponents spectrum in Figure 2b.

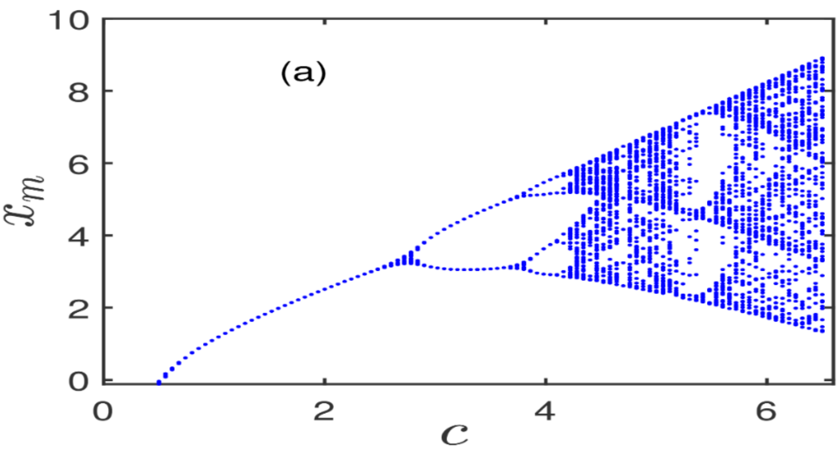

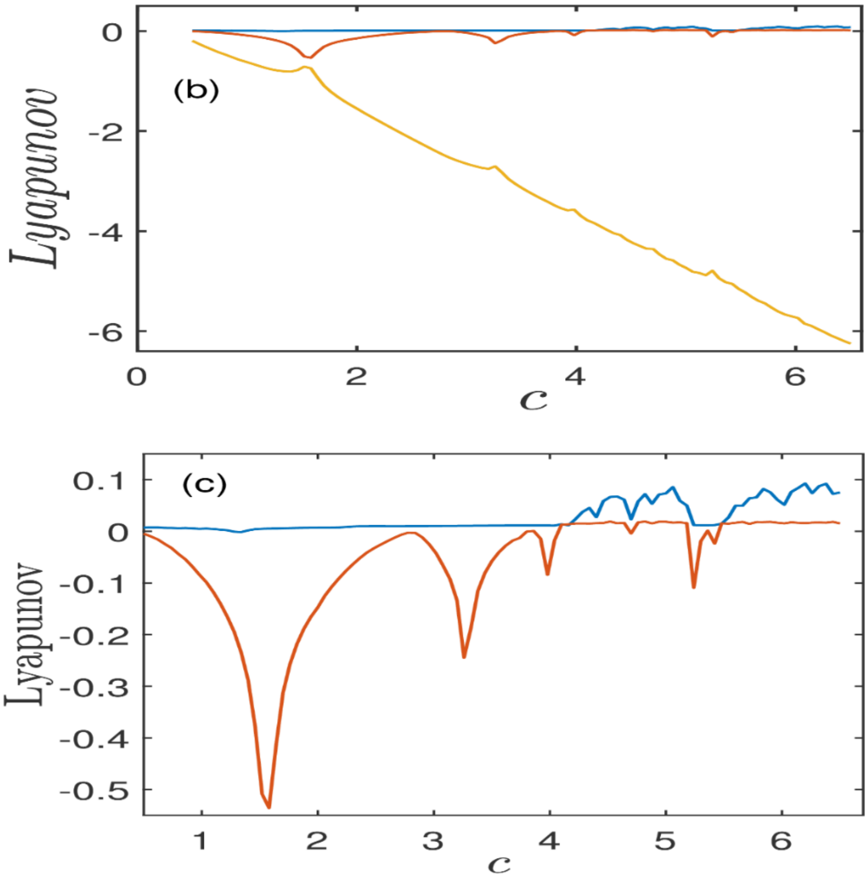

Figure 2: Bifurcation diagram and the Lyapunov exponent spectrum of Equation (1) with varying c when parameters $a = b = 0.2$

Application to a Secure Communication Scheme
This section introduces a secure communication strategy where the parameter of the chaotic drive system is modulated by the input signal to be conveyed. Figure 3 shows the block diagram. Through a public channel, the effective chaotic input signal is conveyed. The controller is activated when switch S is closed; otherwise, it is deactivated.

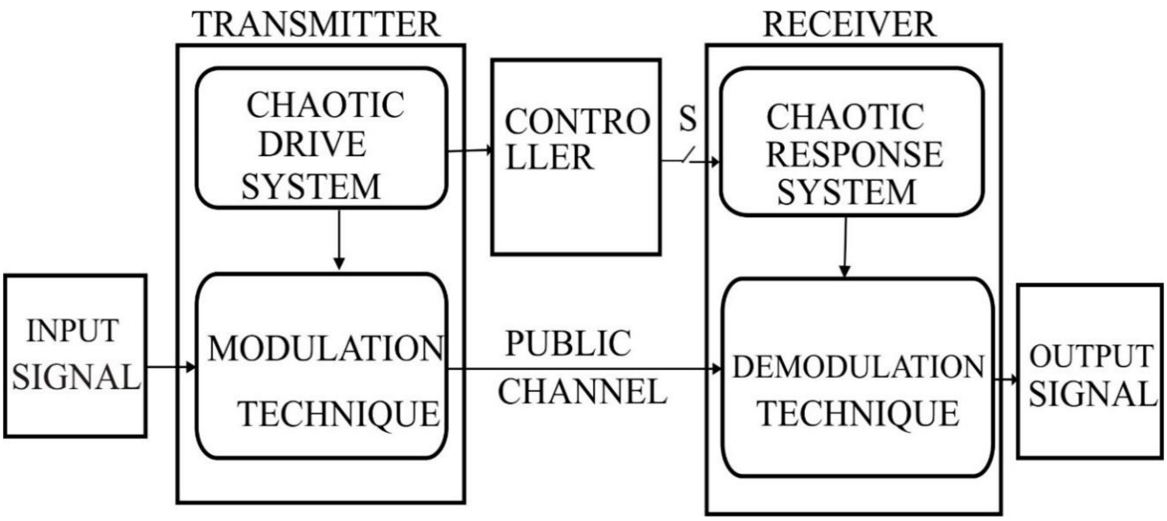

Figure 3: Block diagram of the chaotic communication system

Modulation Technique
A superposition of sinusoidal waves can be used to express any type of electromagnetic signal. The function $s(t) = A\,sin(2\pi f t + \phi)$ represents a general sinusoidal signal, where A represents the amplitude (often expressed in volts), f represents the frequency, and ϕ represents the phase difference. We conceal the original message $s(t)$ into the parameter c of Equation (1). For $c_1 \leq c \leq c_2$, where $c_1 = 4.5$ and $c_2 = 5.1$, Equation (1) is chaotic in this range. Also, we consider a new parameter $\sigma(t)$, such that $\sigma(t) \in [4.5 \quad 5.1]$, and employ the modulation technique in Olusola *et al.* (2020), thus:

$$\sigma(t) = \frac{c_2 - c_1}{\pi} tan^{-1}(s(t)) + \frac{c_2 + c_1}{2}$$
$$\sigma(t) = \frac{0.6}{\pi} tan^{-1}(s(t)) + 9.6. \quad (6)$$

Design of the Controller

Firstly, to design a suitable controller, parameter c in Equation (1) is replaced by the new parameter $\sigma(t)$ to obtain:
$$\begin{cases} \dot{x}_1 = -(x_2 + x_3) \\ \dot{x}_2 = x_1 + ax_2 \\ \dot{x}_3 = b + x_3(x_1 - \sigma(t)). \end{cases} \quad (7)$$
Equation (7) is hereafter referred to as the transmitter system. The receiver system is describable by the following equation:
$$\begin{cases} \dot{y}_1 = -(y_2 + y_3) + u_1 \\ \dot{y}_2 = y_1 + ay_2 + u_2 \\ \dot{y}_3 = b + y_3(y_1 - \hat{\sigma}(t)) + u_3, \end{cases} \quad (8)$$
where $\hat{\sigma}(t)$ is an unknown parameter to be estimated; and $u_i (i = 1,2,3)$ are the controllers to be designed. The design of the controller is done in such a way that: (i) the transmitter system and the receiver system achieve hybrid synchronization; (ii) the parameters $\sigma(t)$ and $\hat{\sigma}(t)$converge to the same value.

Active control method is employed to examine the hybrid synchronization. This is done by defining the system error, parameter error and time derivative of error signals as follows:
$$\begin{cases} e_1 = y_1 - k_1 x_1 \\ e_2 = y_2 + k_2 x_2 \\ e_3 = y_3 - k_3 x_3, \end{cases} \quad (9)$$
where k_i $(i = 1,2,3)$, is the scaling factor. For simplicity, k_i is taken as unity in this work.

Also,
$$e_\sigma = \hat{\sigma}(t) - \sigma(t). \quad (10)$$
The time derivative of Equation (9) is:
$$\begin{cases} \dot{e}_1 = \dot{y}_1 - k_1 \dot{x}_1 \\ \dot{e}_2 = \dot{y}_2 + k_2 \dot{x}_2 \\ \dot{e}_3 = \dot{y}_3 - k_3 \dot{x}_3. \end{cases} \quad (11)$$
Substituting Equations (7) and (8) into Equation (11) yields:
$$\begin{cases} \dot{e}_1 = -(e_2 + e_3) + 2x_2 + u_1 \\ \dot{e}_2 = e_1 + ae_2 + 2x_1 + u_2 \\ \dot{e}_3 = e_1 e_3 + e_3 x_1 + e_1 x_3 - \hat{\sigma}(t) e_3 + u_3. \end{cases} \quad (12)$$
Also, taking the time derivative of parameter estimate error leads to:
$$e_\sigma = \hat{\sigma}(t) - \frac{0.6}{\pi(1+s^2(t))}. \quad (13)$$
Hence, the hybrid synchronization problem becomes the stability problem of the error dynamics, Equation (13). We obtain the following theorem:

The theorem: From Equations (12) and (13), hybrid synchronization between the transmitter system and the receiver system can be realized when the control function, u_i and the parameter update law are selected thus:
$$\begin{cases} u_1 = -2x_2 + w_1 \\ u_2 = -2x_1 + w_2 \\ u_3 = -e_1 e_3 - e_3 x_1 - e_1 x_3 + w_3, \end{cases} \quad (14)$$
where $w_1 = e_2 + e_3, w_2 = -e_1 - ae_2, w_3 = \hat{\sigma}(t) e_3$.

and
$$\hat{\sigma}(t) = \frac{0.6}{\pi(1+s^2(t))}, \quad (15)$$
Proof: Let us consider:
$$W = [w_1, w_2, w_3]^T = A[e_1, e_2, e_3]^T, \quad (16)$$
where $W = [w_1, w_2, w_3]^T$ are the linear control input chosen such that the system becomes stable, then the transmitter and the receiver will achieve stable hybrid synchronization. Also, A is a 3×3matrix. The matrix A should be chosen in such that all its eigenvalues have negative real parts. Consider the following choice of A:
$$A = \begin{vmatrix} -1 & 1 & 1 \\ -1 & -(1+a) & 0 \\ 0 & 0 & (\hat{\sigma}(t) - 1) \end{vmatrix}, \quad (17)$$
then, Equation (16) becomes:
$$[w_1, w_2, w_3]^T = \begin{vmatrix} -1 & 1 & 1 \\ -1 & -(1+a) & 0 \\ 0 & 0 & (\hat{\sigma}(t) - 1) \end{vmatrix} \begin{vmatrix} e_1 \\ e_2 \\ e_3 \end{vmatrix}. \quad (18)$$
Substituting the solution of Equation (18) in Equation (14) yields:
$$\begin{cases} u_1 = -e_1 + e_2 + e_3 - 2x_2 \\ u_2 = -e_1 - (1+a)e_2 - 2x_1 \\ u_3 = -e_1 e_3 - e_3 x_1 - e_1 x_3 - (1 - \hat{\sigma}(t)) e_3. \end{cases} \quad (19)$$
Based on the Lyapunov second method, we construct a Lyapunov function:
$$V(e_1, e_2, e_3) = \frac{1}{2} \sum k_i e_i^2. \quad (20)$$
By calculating the derivative of $V(t)$ along the trajectories of the error system (12) with k_i $(i = 1,2,3)$ being unity (as stated before),
$$\dot{V}(t) = e_1 \dot{e}_1 + e_2 \dot{e}_2 + e_3 \dot{e}_3 \quad (21)$$
Using Equations (12) and (19) in Equation (21) gives:
$$\dot{V}(t) = e_1(-e_1) + e_2(-e_2) + e_3(-\hat{\sigma}(t) e_3),$$
$$\dot{V}(t) = -e_1^2 - e_2^2 - \hat{\sigma}(t) e_3^2,$$
$$\dot{V}(t) < 0. \quad (22)$$
As the time, t, tends to ∞, the error function tends to zero; that is, hybrid synchronization between the transmitter system and the receiver system is achieved, and the zero point of the parameter error e_σ is globally and asymptotically stable. This result makes it clear that the derivative of the Lyapunov function is negative definite. It implies that the uncertain parameter $\sigma(t)$ is also estimated in the receiver simultaneously. This completes the proof.

Demodulation

As the hybrid synchronization between the transmitter system and the receiver system appears, one can identify the parameter $\hat{\sigma}(t)$.

Consequently, from the invertible transformation Equation (6), the original message signal can be recovered as:
$$r(t) = tan\left(\frac{\pi}{0.6}(\hat{\sigma}(t) - 9.6)\right). \quad (23)$$
Here $r(t)$ represents the recovered signal. Therefore, the receiver can successfully extract the message signal from $\hat{\sigma}$ by this demodulation technique.

RESULTS AND DISCUSSION

Numerical simulations were performed using the ODE45 algorithm embedded in MATLAB to show the feasibility and effectiveness of this communication scheme. The parameter values are $a = b = 0.2$ $\hat{\sigma}(t) = [4.5 \ \ 5.1]$ with initial conditions $x_1(0) = -0.1$, $x_2(0) = -0.1$, $x_3(0) = 0.3$ and $y_1(0) = -0.2$, $y_2(0) = 0.3$, $y_3(0) = -0.1$. The control gains $k_1 = k_2 = k_3 = 1$. Equation (1) remains chaotic with this choice of parameter values. The hybrid synchronization errors between the transmitter system and the receiver system are depicted in Figures 4 and 5.

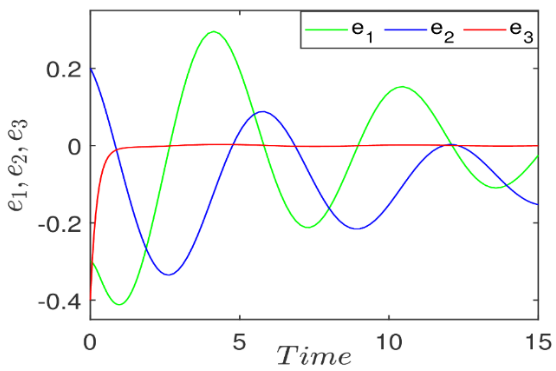

Figure 4: The hybrid synchronization error of the transmitter system and the receiver system before the controller is activated

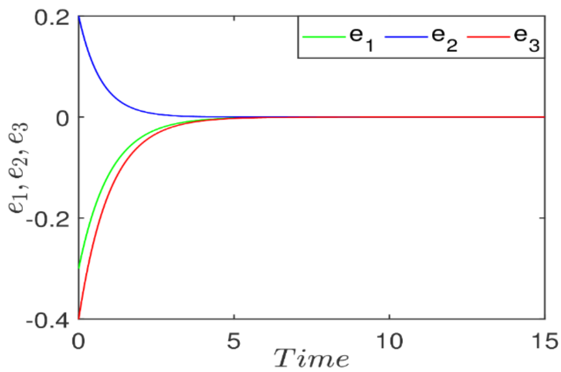

Figure 5: The hybrid synchronization error of the transmitter system and the receiver system after the controller is activated

Figure 4 depicts the hybrid synchronization error of the transmitter system and the receiver system before the controller is activated; while Figure 5 shows the hybrid synchronization error of the transmitter system and the receiver system after the controller is activated. It is evident that after the designed controllers were activated, the coupled transmitter system and the receiver system become asymptotically stable at time, $t \geq 5$. This validates the feasibility and effectiveness of the designed controller.

For the message signal, $s(t) = A\,sin(2\pi ft + \phi)$, hidden in the transmitter, one readily obtain

$$\sigma(t) = \frac{0.6}{\pi} tan^{-1}(A\,sin(2\pi ft + \phi)) + 9.6. \qquad (24)$$

The message, $s(t)$, was embedded in the parameter $\sigma(t)$of the transmitter system (Equation (7)) which resulted into the phase portrait shown in Figure 6 with the following choice of parameters: $A = 22V, f = 50Hz$ and $\phi = 45^0$.

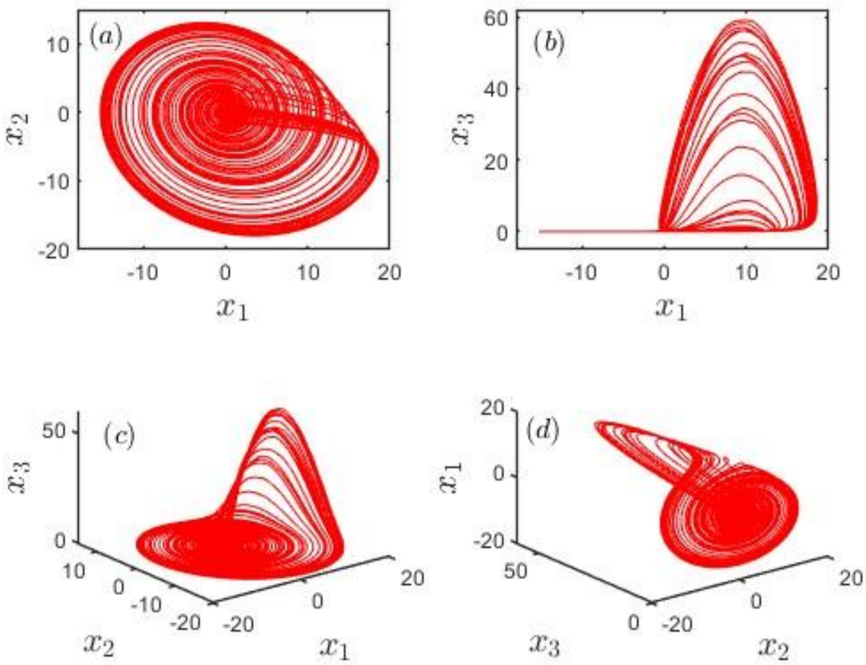

Figure 6: Phase portrait of the Rossler attractor after the message was embedded with the following parameters $a = 0.2, b = 0.2, c = 5.7, A = 22V, f = 50Hz, \phi = 45^0$

As expected, the transmitted message slightly affected the phase portrait of the Rossler system. The chaotic massage was received by the receiver and identified as $r(t)$ in the demodulation stage (Equation (23).

The signal paths of the sent message signal and the recovered message signal are depicted in Figures 7 to 9.

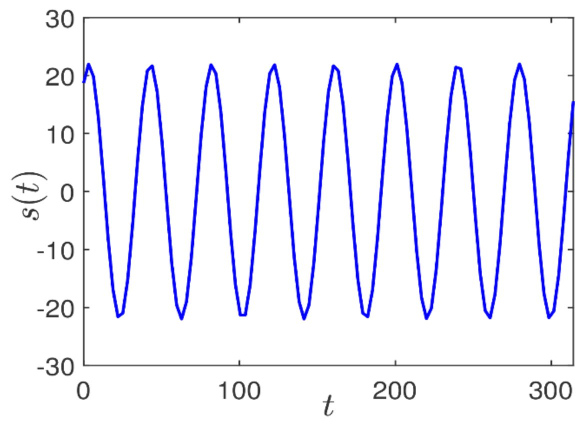

Figure 7: The original message signal $s(t)$

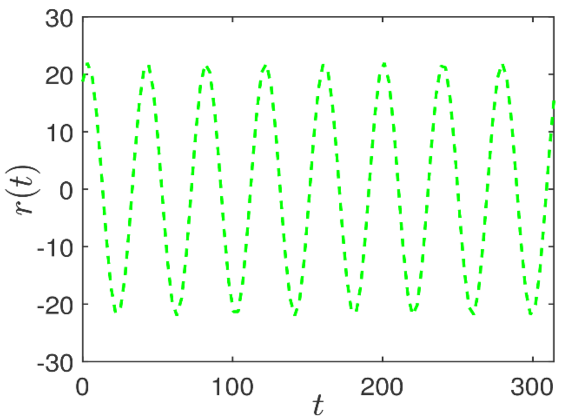

Figure 8: The recovered message signal $r(t)$. Figure 7 and Figure 8 show the signal paths of the sent message signal and the recovered message signal respectively

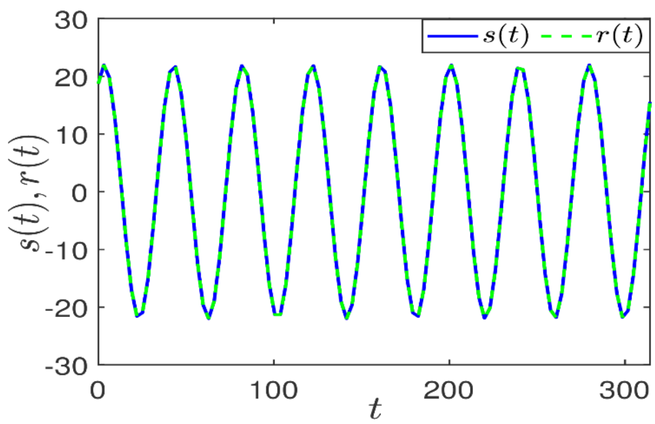

Figure 9: The original message signal $s(t)$ and the recovered message signal $r(t)$

The correlation between the recovered message signal and the original message signal is clearly shown in Figure 8. Thus, the desired secure communication goal is accomplished, and the message signal is accurately received.

CONCLUSION

This work has presented a secure communication strategy that is achieved via a minimal continuous chaos system. When the designed controllers are activated, they are capable of making the time derivative of the Lyapunov function negative definite, which ensures the stability of the error dynamics and, consequently, the synchronization of the systems. This scheme allows the message signal to be successfully and secretly passed through four main paths: modulation, chaotic transmitter, chaotic receiver, and demodulation. Finally, the presented communication scheme was subjected to numerical simulations to prove its effectiveness and feasibility.

ACKNOWLEDGMENTS

We appreciate the expertise of the reviewer, whose comments and suggestions improved the overall quality of our manuscript.

REFERENCES

Benkouider, K., Sambas, A., Sulaiman, I. M., Mamat, M., & Nisar, K. S. (2002). Secure communication scheme based on a new hyperchaotic system. *Computers, Materials and Continua*, **73** (1), 1019–1035.

Boccaletti, S., Kurths, J., Osipov, G., Valladares, D., & Zhou, C. (2002). The ynchronization of chaotic systems. *Physics Reports*, **366** (1), 1-101.

Bouraoui, H., & Kemih, K. (2013). Observer-based synchronization of a new hybrid chaotic system and its application to secure communications. *Acta Physica Polonica A*, **123**, 259-262.

Cuomo, K. M., & Oppenheim, A. V. (1993). Circuit implementation of synchronized chaos with applications to communications. *Phys. Rev. Lett.*, **71,** 65-68.

Gaspard, P., & Bricmont, J. (1999). Chaos, scattering and statistical mechanics. *Physics Today*, **52**(8), 62-64.

Gosar, Z. (2011). Chaotic dynamics – Rossler system. *Researchgate*, 10 doi:10.13140/RG.2.2.27897.62564.

Kocarev, L., & Parlitz, U. (1995). General approach for chaotic synchronization with applications to communication. *Phys. Rev. Lett.*, **74**, 5028-5031.

Li, Z., Li, K., Wen, C., & Soh, Y. C. (2003). A new chaotic secure communication system. *IEEE Trans. Commun.*, **51**, 1306-1312.

Li, Z., & Xu, D. (2004). A secure communication scheme using projective chaos synchronization. *Chaos, Solitons and Fractals*, **22**(2), 477–481.

Lu, Q. S., Gu, H. G., Yang, Z. Q., Shi, X., Duan, L., & Zheng, Y. (2008). Dynamics of firing patterns, synchronization and resonances in neuronal electrical activities: experiments and analysis. *Acta Mechanics Sinica*, **24**, 593–628.

Miliou, A. N., Antoniades, I. P., Stavrinides, S. G., & Anagnostopoulos, A. N. (2007). Secure communication by chaotic synchronization: Robustness under noisy conditions. *Nonlinear Analysis: Real World Applications*, **8**, 1003-1012.

Ni-huan, L., & Zhi-hong, H. (2012). A hybrid secure communication method based on the synchronization of hyperchaos systems. *International Conference on Communication Systems and Network Technologies*, 289-293.

Olusola, O. I., Oyeleke, K. S., Vincent, U. E., & Njah, A. N. (2020). Secure communication scheme based on synchronization of non-identical hyperchaotic systems. *Journal of Applied Nonlinear Dynamics*, **9** (2), 273-285.

Pecora, L. M., & T. L. Carroll. (1990). Synchronization in chaotic systems. *Phys. Rev. Lett.*, **64**, 821-824.

Rai, A., Joshi, M., Upadhyay, K. K., Jyoti, V. K., Shastri, H., & Goyal, S. (2023). Realization of chaotic oscillator and use in secure communication. *e-Prime - Advances in Electrical Engineering, Electronics and Energy*, **6**, 100321.

Rosenblum, M. G., Pikovsky, A. S., & Kurths, J. (1996). Phase synchronization of chaotic oscillators. *Phys. Rev. Lett.*, **76**, 1804-1807.

Rossler, O. E. (1976). An equation for continuous chaos. *Physics Letters A*, **57**(5), 397-398.

Rulkov, N. F., & Tsimring, L. S. (1999). Synchronization methods for communication with chaos over band-limited channels. *International Journal of Circuit Theory and Applications*, **27**(6), 555-567.

Samimi, M., Majidi, M. H., & Khorashadizadeh, S. (2020). Secure communication based on chaos synchronization using brain emotional learning. *AEU - International Journal of Electronics and Communications*, **127**, 153424.

Trikha, P., & Jahanzaib, L. (2021). Secure communication: Using double compound combination hybrid synchronization. *Proceedings of International Conference on Artificial Intelligence and Applications*, 81-91.

Wu, X., Yao, C., & Shuai, J. (2015). Enhanced multiple vibrational resonances by Na^+ and K^+ dynamics in a neuron model. *Scientific reports*, **5**, 7684.

Yau, H., Pu, Y., & Li, S. (2012). Application of a chaotic synchronization system to secure communication. *Information Technology and Control*, **41**(3), 274-282.

Yeh, J., & Wu, K. (2008). A simple method to synchronize chaotic systems and its application to secure communications. *Mathematical and Computer Modelling*, **47**(9), 894-902.

Zaher, A., & Abu-Rezq, A. (2011). On the design of chaos-based secure communication systems. *Communications in Nonlinear Science and Numerical Simulation*, **16**, 3721-3737.

Zhao, Y. Li, S. Lian, H., & Wu, Z. (2014). A six-dimensional hyperchaotic system selection and its application in DS-CDMA system. *Journal of Communications*, **9**(11), 859-866.

Zheng, Z., & Hu, G. (2000). Generalized synchronization versus phase synchronization. *Phys Rev. E*, **62**, 7882-7885.